Title: Plasticity of gene expression in the nervous system by exposure to environmental odorants that inhibit HDACs

AUTHORS: Sachiko Haga-Yamanaka[*,1], Rogelio Nuñez-Flores[*,1,5], Christi Ann Scott[*,2], Sarah Perry[3], Stephanie Turner Chen[2], Crystal Pontrello[1], Meera Goh Nair[5] and Anandasankar Ray[1,2,3]

ADDRESS:

[1]Department of Molecular, Cell and Systems Biology

[2]Cell, Molecular and Developmental Biology Program

[3]Genetics, Genomics and Bioinformatics Program

[4]Department of Nematology

[5]Division of Biomedical Sciences

University of California, Riverside, CA 92521, USA

* these authors contributed equally

CORRESPONDING AUTHOR: Anandasankar Ray

Department of Molecular Cell and Systems Biology, University of California Riverside, 3401 Watkins Drive, Riverside, CA 92521, USA

CONTACT INFORMATION : Phone : +1(951) 827-5998, Email : anand.ray@ucr.edu

ABSTRACT

Eukaryotes are often exposed to microbes and respond to their secreted metabolites, such as the microbiome in animals or commensal bacteria in roots. Little is known about the effects of long-term exposure to volatile chemicals emitted by microbes, or other volatiles that we are exposed to over a long duration. Using the model system *Drosophila melanogaster,* we evaluate a yeast emitted volatile, diacetyl, found in high levels around fermenting fruits where they spend long periods of time. We find that exposure to just the headspace containing the volatile molecules can alter gene expression in the antenna. Experiments showed that diacetyl and structurally related volatile compounds inhibited human histone-deacetylases (HDACs), increased histone-H3K9 acetylation in human cells, and caused wide changes in gene expression in both *Drosophila* and mice. Diacetyl crosses the blood-brain barrier and exposure causes modulation of gene expression in the brain, therefore has potential as a therapeutic. Using two separate disease models known to be responsive to HDAC-inhibitors, we evaluated physiological effects of volatile exposure. First, we find that the HDAC inhibitor also halts proliferation of a neuroblastoma cell line in culture as predicted. Next, exposure to vapors slows progression of neurodegeneration in a *Drosophila* model for Huntington's disease. These changes strongly suggest that unbeknown to us, certain volatiles in the surroundings can have profound effects on histone acetylation, gene expression and physiology in animals.

INTRODUCTION

Multicellular organisms evolve in the presence of microbial volatiles and metabolites (1, 2), often for prolonged periods of time. Human-associated microbes have incredible metabolic diversity, encoding 100x as many genes as the human genome itself(1). It is estimated that about half of the thousands of metabolites found in mammalian blood are either produced or altered by microbes (3). Microbial metabolites are an important mechanism by which the microbiome influences host immunity amongst other things (2, 4). Many volatiles are generated from the metabolism of a variety of food components, including triglycerides, sugars and amino acids (5). Some chemicals are also produced by microorganisms such as yeasts and lactic bacteria during fermentation in many foods and beverages (5).

In the model system *Drosophila melanogaster*, prolonged exposure to CO_2 showed an increase in volume of the CO_2-sensing glomerulus in the antennal lobe, which can lead to adaptations in fly behavior (6, 7, 8). Carbon dioxide is a common byproduct of yeast fermentation in overripe fruits, the preferred food source. In order to study the physiological effects of long-term exposure to other volatiles emitted during fermentation, we exposed flies for 5 days to diacetyl, a buttery odorant made at high levels by yeast in fermenting fruits (1350 ppb in ripe banana), that is also found in many commonly consumed foods such as butter, yoghurt, wine, fruits, beer, popcorn (5, 9-11). Diacetyl was selected for two reasons: first, *Drosophila melanogaster* use fermenting fruits as their favored food source, oviposition site and spend long durations of time exposed to it. Second, diacetyl is known to be an inhibitory odorant of the CO_2 receptor and therefore an opposite effect is expected on the V-glomerulus from the previous study (12). Follow up experiments revealed that diacetyl acts as an HDAC inhibitor in vitro. We found that volatiles structurally like diacetyl have similar HDAC-inhibitory properties as well.

73 Subsequent analyses with two different model systems: *Drosophila melanogaster* and *Mus*
74 *musculus* showed gene expression changes in tissues caused by odor exposure from a distant
75 source. We found expression of hundreds of genes to be modulated upon exposure to the volatile,
76 as would be expected from an inhibitor of HDACs. HDACs are histone-modifying enzymes
77 involved in the removal of acetyl groups from lysine residues and the remodeling of chromatin
78 structure to regulate gene expression (13, 14). With large-scale roles in gene regulation, HDACs
79 are promising targets in drug development for many diseases such as cancers and
80 neurodegenerative disorders (15-17). Several classes of orally administered HDAC inhibitors have
81 been found to attenuate the progression of certain cancers and neurodegenerative diseases
82 including Alzheimer's disease and Huntington's disease (17). We determined that exposure to
83 diacetyl volatiles substantially altered gene expression in the mouse brain, presumably by crossing
84 the blood-brain barrier. Diacetyl exposure also slowed degeneration of photoreceptor cells in a
85 Huntington's disease model in *Drosophila*. Last, exposure to diacetyl caused dramatic reduction
86 in proliferation of a neuroblastoma cell line in culture. Our discovery of a family of volatile
87 odorants that also act as HDAC inhibitors highlights the need to understand how small molecules
88 present in our environment interact with and alter eukaryotic gene expression.

89 **RESULTS**

90 **Activity-dependent expression modulation of chemosensory receptors**

91 Previous studies demonstrated that prolonged exposure of ~5 days to elevated CO_2,
92 causes an increase in volume of the CO_2-sensitive V-glomerulus in the antennal lobe, which can
93 lead to adaptations in fly behavior (6, 7, 8). To assess the effect of CO_2 response inhibitor
94 diacetyl on the antennal lobe, flies were exposed to the odorant during the first days immediately

95 following eclosion. The CO_2-detecting ab1C neuron was labelled using the promoters of the CO_2
96 receptors, *Gr63a-Gal4; UAS-mcd8GFP* and *Gr21a-Gal4; UAS-mcd8GFP*, and the flies were
97 exposed to headspace above a 1 % (V/V) diacetyl solution in an air-tight container. The flies
98 were then imaged for expression of GFP in the ab1C neurons of the antenna, as well as the V
99 glomerulus, which receives axonal input from ab1C neurons in the antennal lobe (18).
100 Surprisingly, the *Gr63a* promoter driven GFP signal in the V glomerulus was completely
101 abolished after 5 days of exposure to the odor for all brains imaged (Figure 1A,1B). However,
102 there was also a concomitant decrease in GFP signal in ab1C neurons in the antenna (Figure 1A).
103 Similar results were seen for *Gr21a* driven expression, where expression of GFP was lost in both
104 the V-glomerulus and ab1C neurons (Figure S1A, S1B). Interestingly, after five days of recovery
105 in clean air the GFP expression was regained in the V-glomerulus as well as in ab1C neurons in
106 the antenna, indicating that both *Gr21a* and *Gr63a* expression had been restored (Figure S2).
107 Because olfactory neurons do not regenerate in the fruit fly (19, 20), these results suggest that
108 changes in GFP levels are likely due to changes in the promoter expression and not due to
109 neuronal cell death.

110 In order to test whether expression of *Gr63a* and *Gr21a* is being downregulated by
111 diacetyl we relied on quantitative-PCR along with a few members of the *Odorant receptor (Or)*
112 family genes. Apart from *Gr63a* and *Gr21a,* we also evaluated receptors where diacetyl has no
113 activity (*Or47a*, *Or88a*) and the broadly expressed co-receptor (*Or83b*). Wild-type flies that
114 were exposed to diacetyl for 6 days showed dramatic downregulation of all genes tested.
115 However, after a 5-day recovery period, expression of all but one (*Or88a*) of the genes was
116 recovered, including *Gr63a* (Figure S1C). This form of plasticity in gene expression is
117 unexpected and therefore mechanistically interesting to investigate.

118 **Diacetyl and structurally related odorants act as HDAC inhibitors in vitro**

119 Diacetyl is structurally related to the soluble metabolite secreted by the gut microbiome
120 and liver, β-hydroxybutyrate, which is known to inhibit zinc-dependent HDACs (21). It is also
121 structurally related to another known HDAC inhibitor Sodium butyrate. Diacetyl is present widely
122 in nature as a pH-neutral fermentation product of microorganisms such as yeasts in over-ripe fruit,
123 the favorite food for *Drosophila*, and also from lactic acid bacteria, and is found in many foods
124 and beverages (5). In humans, diacetyl is also produced by microbes on the skin, in the oral cavity,
125 and is found in breath (22). Interestingly, this volatile is known to traverse the cell membrane (23).

126 Soluble metabolites from the gut microbiome, such as short chain fatty acids, are known
127 to affect histone modifying enzymes, gene expression, and physiology in various parts of the host
128 (1, 24). It is presumed that these dissolved compounds absorbed in the blood circulate to various
129 parts of the body. Microbes in our skin microbiome, mouth microbiome, and environment also
130 emit a diverse repertoire of volatile metabolites that can traverse much greater distances away from
131 the source (25). To examine if diacetyl can directly modulate HDACs like β-hydroxybutyrate, we
132 performed in vitro acetylation assays with recombinant human HDACs. We found that indeed,
133 diacetyl inhibited all four purified human Class I HDACs (HDAC1, 2, 3 and 8) and the one Class
134 II HDAC (HDAC6) tested. The inhibition occurred in a dose-dependent manner. The IC_{50} values
135 for HDAC1, 2, 3, 8 and 6 were 7.3 mM, 23.1 mM, 7.5 mM, 14.3 mM, and 24.5 mM respectively
136 (Figure 1C). The levels of inhibition as observed from IC_{50} values for HDAC1 and HDAC3 were
137 comparable to those of β-hydroxybutyrate whose IC_{50} values for HDAC1 and 3 were previously
138 reported as 5.3 and 2.4 mM, respectively (21).

139 To test other odorants for their ability to inhibit HDACs, we identified a list of volatile
140 odorants structurally similar to diacetyl using the similarity search feature on PubChem (Figure
141 1D) and are volatile and tested them on four purified human HDACs, from Class I (HDAC1 and
142 HDAC3) and Class II (HDAC4 and HDAC6). Each compound was tested at 15 mM, the
143 concentration at which diacetyl inhibits HDAC1, 3, and 6 with more than 50% efficacy (Figure
144 1C, D). All compounds tested reduced the activity of at least one of the HDACs (Figure 1D). Ethyl
145 pyruvate, methyl pyruvate, 2,3-hexanedione, 2,3-heptandione, 2,3-pentandione inhibited HDAC1,
146 3 and 6 with more than 70% efficacy. Allyl butyrate also similarly inhibited those HDACs but
147 with lower efficacy. 1-acetoxyacetone, and 2,3-butanediol inhibited HDAC6 more than 70% but
148 inhibitory effects against HDAC1 and 4 were lower. Moreover, propyl formate strongly inhibited
149 HDAC 6 but did not inhibit HDAC1, 3, and 4. Taken together, these results indicate that microbial
150 volatiles and structurally related odorants can inhibit human HDACs, and that each compound has
151 specific HDAC inhibitory properties.

152 **Microbial volatile increases histone acetylation in human cell nuclei**

153 In order to directly examine histone acetylation at the cellular level, we used human
154 HEK293 cells, which offer a tractable system to prepare nuclear extracts, and picked the volatile
155 diacetyl to test in more detail. We exposed the cells to different doses of diacetyl for 2 or 6 hours
156 and monitored histone acetylation levels within nuclear extracts in Western Blot assays. Compared
157 to the mock treatment, 10 mM diacetyl significantly increased H3K9 acetylation levels within 2
158 hours of treatment, whereas the acetylation levels of H3K14 and H4K5 were not affected (Figure
159 2A). This specificity for an increase of the H3K9 mark is consistent with previous observations
160 for β-hydroxybutyrate. Preferential acetylation of H3K9 was also observed previously in HEK293
161 cells with treatment of the structurally related β-hydroxybutyrate (21). After 6 hours of treatment,

162 the H3K9 acetylation induced by 10 mM diacetyl was further increased (Figure 2B). The increase
163 in H3K9 acetylation with diacetyl treatment was dependent both on the duration of exposure and
164 concentration of the odorant.

165 Organisms are constantly exposed to volatiles commonly found in their food and
166 environment for prolonged periods of time. In order to test the effect of a lower concentration of
167 the volatiles, we selected a 5-day exposure time at a 100-fold lower concentration. When we
168 treated HEK293 cells with this lower dose of diacetyl (100 μM), H3K9 acetylation level increased
169 after 96 hours of exposure and reached significantly higher levels than control after 120 hours
170 (Figure 2C,D). These results demonstrate that even prolonged exposure to low levels of diacetyl
171 can greatly impact the epigenetic landscape inside the nucleus. More importantly, a 5-day exposure
172 was sufficient to alter the epigenetic state of nuclei at concentrations that are present in some food
173 sources. Taken together, these results demonstrate that diacetyl can act as an HDAC inhibitor, with
174 the potential of causing broad modulations of gene expression and histone acetylation in cells.

175 **Transcriptional response to odor exposure is conserved in invertebrates and vertebrates**

176 We next performed in vivo experiments to determine whether eukaryotic cells alter gene
177 expression in response to diacetyl exposure, as would be expected with HDAC-inhibition.
178 Epigenetic changes occur slowly over days, and to test its effects on gene expression we used two
179 model systems for eukaryotes: invertebrates (*Drosophila melanogaster)* and vertebrates *(Mus*
180 *musculus).* We placed *Drosophila* adult males in vials and housed these vials within a closed
181 container exposed to headspace from a 1% diacetyl solution (in paraffin oil) for 5 days, similar to
182 a previous long-term odor-exposure study (7) (Figure 3A). The transcriptome of the primary
183 olfactory organ, the antenna, was compared with that of the control group of age-matched flies

184 that were exposed to the solvent paraffin oil (PO). The antennal transcriptional profile of diacetyl-
185 exposed flies showed substantial changes in gene expression when compared to the solvent control
186 (Figure 3B). We identified 1234 differentially expressed genes (DEGs) (false discovery rate, FDR
187 < 0.05) in the antennal transcriptome of diacetyl-exposed flies compared to control animals. Of
188 these, 645 genes were significantly up-regulated ($\log_2$ fold-change > 1; red dots in Figure 3B) and
189 589 genes were significantly down-regulated ($\log_2$ fold-change < -1; blue dots in Figure 3B). A
190 broad range of genes was significantly altered, with several biological process GO terms
191 significantly enriched in the up-regulated gene list including "response to biotic stimulus" ($p <$
192 $3x10^{-7}$),"response to bacterium" ($p < 3x10^{-7}$) and "defense response" ($p < 3x10^{-7}$). In the down-
193 regulated gene set the GO term most enriched was "sensory perception of chemical stimulus" ($p<$
194 $6x10^{-72}$). The GO molecular functions that were most common in the upregulated sets included
195 enzymes like hydrolases and oxidoreductases, as well as nucleic acid binding genes (Figure 3C).
196 Down-regulated genes include receptors, hydrolases, and transporters (Figure 3C).

197 The first tissue that would have contact with airborne volatiles in terrestrial vertebrates are
198 the airways and lungs. We therefore performed transcriptome analyses on lung tissue of mice
199 exposed to diacetyl headspace at different doses for a period of 5 days, as was done in *Drosophila*
200 (Figure 3D). The dose of the volatile in the chamber was measured in parallel experiments by
201 tracking volatile loss and airflow and determined to range between a peak 1920 ppm at the end of
202 hour 2, tapering off to 28 ppm by hour 120 (Supplemental Figure S3B). Indeed, expression of a
203 substantial number of genes was modulated in the diacetyl-exposed lungs compared to the control.
204 The changes were dose-dependent and more pronounced in mice exposed to headspace from a 1%
205 diacetyl source compared to those exposed similarly to 0.1% (v/v) diacetyl source (Figure 3E,
206 Supplemental Figure S3C). Among these diverse sets of regulated genes in the lung tissue, a

207 significant overlap was found between 1% (v/v) and 0.1% (v/v) headspace for both up-regulated
208 genes ($p=3x10^{-3}$) and down-regulated genes ($p=6x10^{-3}$, Figure 4F), further supporting a dose-
209 dependent effect of diacetyl on gene expression in the mouse lung.

210 The GO enrichment analysis of the lung transcriptome from mice exposed to diacetyl
211 revealed several interesting sets of genes that were significantly altered (Figure 3G,H). Among
212 these genes is the SARS-CoV-2 entry receptor ortholog, ACE2. The level of this gene in the lungs
213 of diacetyl exposed mice showed a reduction in expression levels (log_2 fold-change= - 0.62, FDR=
214 $2.02x10^{-5}$). The level of ACE2 in the nasal tissue, lungs and other organs play a critical role in
215 infection by the SARS-CoV-2 virus, suggesting that epigenetic mechanisms may contribute to
216 expression. While we do not know whether expression of ACE2 in humans is regulated similarly,
217 these results highlight the importance of understanding volatile-induced modulation of gene
218 expression in the lungs and other tissues.

219 HDAC family members are highly conserved across eukaryotes, spanning both animal and
220 insects. Volatile microbial metabolites have been present throughout the evolution of animals,
221 insects, and plants, and have potential as signals for multi-domain communication because they
222 can travel wide ranges; plants detect root infections and time their immune response using volatiles
223 (26), and microbial volatiles elicit olfactory behaviors in insects and nematodes. Our results
224 indicate that a volatile compound, capable of directly inhibiting HDACs and altering acetylation
225 levels, can cause significant changes in gene expression in a variety of organisms following
226 exposure from a distance, through the air.

227 **DEGs overlap those for known HDAC inhibitors and upregulation is partially reversible**

228 One of the hallmarks of epigenetic regulators which makes them attractive candidates for
229 therapeutics is plasticity. Upon removal of the inhibitors, we expect that some of the changes in
230 gene expression are reversible. To test for reversibility, we performed a recovery experiment
231 following diacetyl exposure using the *Drosophila* model. We maintained 5-day diacetyl-exposed
232 flies in clean air for 5 additional days (Figure 4A). In parallel, we performed age-matched mock
233 experiments with paraffin oil solvent exposure alone. A large number of genes were down-
234 regulated following the recovery in comparison to the 10-day-old flies in the mock condition
235 (Figure 4B). Interestingly, there was a significant overlap of these down-regulated genes with the
236 set that was up-regulated in the diacetyl treatment (Figure 4C). These results suggest that the
237 effects of HDAC inhibitory odorant exposure are not permanent but dynamic, and removal of the
238 odorant leads to subsequent changes in gene expression of the up-regulated set.

239 Drugs that inhibit HDACs are in various stages of approval as treatments for several
240 diseases. The approved drugs include sodium butyrate and valproic acid. To compare the gene-
241 regulatory effects of these drugs to diacetyl, we performed RNA-seq after raising the flies on food
242 containing sodium butyrate (SB) or valproic acid (VA) (27) and compared gene expression in the
243 antennae of flies raised on untreated food for 5 days. We next compared the up-regulated gene
244 profiles following each treatment to the one induced by exposure to diacetyl. As expected, feeding
245 SB and VA induced significant changes in expression levels of several genes (Figure 4D,E).
246 Interestingly we found that 113 of diacetyl up-regulated genes were also up-regulated in either SB,
247 VA or both treatment conditions (Figure 4F). Pairwise statistical analysis of each gene set revealed
248 a significant overlap of diacetyl-induced genes with SB-induced genes ($p=6x10^{-11}$) and with VA-
249 induced genes ($p=2x10^{-65}$) (Figure 4F). There was, as expected, also a significant overlap between
250 SB- and VA- induced genes ($p=1x10^{-52}$) (Figure 4F). This highly significant overlap among up-

251 regulated genes lends further support to our model that diacetyl vapors act as an HDAC inhibitor
252 in vivo. As expected, each of the 3 treatments also modulated a substantial number of unique genes
253 (Figure 4G, H), suggesting that differences in oral vs. vapor delivery, molecular structure and
254 inhibition profile across the repertoire of HDACs may contribute to differences in gene regulation.
255 These results suggest that some volatile odorants, or the microbes that emit them, may impart
256 therapeutic effects like other HDAC inhibitors from a distance, through the air.

257 **Volatile Diacetyl alters gene expression in the mouse brain**

258 One of the categories of challenging diseases that HDAC inhibitors are being tested for
259 drugs are neurodegenerative diseases (28) where volatile odorants may provide a new class of
260 inhaled therapeutics. A major design challenge for nervous system drugs is the ability to cross the
261 blood-brain barrier. Due to the volatility and small size of volatile odorants, there is a possibility
262 that they could diffuse through the intranasal route to the brain directly (29). We cannot tell *a*
263 *priori* whether odorants like diacetyl can travel across the nasal membrane to the brain. In order to
264 test whether cells in the brain of mice respond when presented with diacetyl vapors from a distance,
265 we used gene expression as the final readout to measure it. We performed RNA-seq experiments
266 on mice exposed only to aroma of diacetyl in the air for 5 days as before. Littermate controls were
267 exposed in a similar manner to the solvent (PO) in the air. Interestingly, several genes were
268 differentially expressed upon exposure to headspace from 0.1% (v/v) diacetyl passaged through
269 the air in the holding cage where it is further diluted (49 up-regulated, 32 down regulated, $|\log_2$
270 fold-change$|$ >1, FDR<0.05) or to headspace from 1% (v/v) diacetyl diluted in the holding cage
271 (748 up-regulated, 1031 down regulated, $|\log_2$ fold-change$|$ >1, FDR <0.05) (Figure 5B,C). GO
272 analysis of the regulated genes in the exposed mouse brain transcriptome revealed several
273 interesting sets of genes were significantly altered in each set (Figure 5E). These results indicate

274 that a volatile odorant like diacetyl can reach the brain in mammals, and presumably alter gene
275 expression in neuronal cells. Although the overall DEG sets were different across the lungs and
276 brain, there was a statistically significant overlap, particularly in the 1% exposure, as would be
277 expected from using the same mechanism of action. There was a highly significant overlap
278 ($p=2x10^{-101}$) between genes upregulated in the brain compared with the lungs (248 of 748), as well
279 as for downregulated genes ($p=3x10^{-163}$; 477 of 1031 genes) (Figure 5D).

280 **Diacetyl prevents proliferation of neuroblastoma cells**

281 Among the significantly downregulated genes was *MYCN*, which is known to show
282 increased expression and plays a central role in many types of cancers, suggesting that epigenetic
283 regulation may affect tumor cells. Broad-spectrum HDAC inhibitors have been approved by the
284 FDA for treatment of a variety of cancers. To test the exciting possibility that a volatile HDAC
285 inhibitor, which affects gene expression in the brain, would have an effect against cancers as well,
286 we performed a cell-based assay. We picked neuroblastoma as a candidate since it has a strong
287 dependence on *MYCN* and develop from fetal adrenal neuroblasts (30). Several genetic and
288 "omics" studies have identified genes that are upregulated in neuroblastomas, some of which are
289 considered to be key causative factors (31). We evaluated the DEGs from the diacetyl-exposed
290 mouse brain transcriptome for several of these key genes. Three of the six key genes identified
291 across multiple studies were significantly altered, two of which were significantly downregulated,
292 *MYCN* (P=2.06E-13, FDR=1.76E-12) and *Alk* (P=3.3E-5, FDR=9.48E-5) (Figure 5F)**.** An
293 unbiased computational study evaluated omics datasets and identified 4 genes that were the best
294 predictors of clinical outcome (32), all of which are significantly different in the brains of the
295 diacetyl exposed mice, strikingly 3 of which were significantly downregulated, *NCAN (p=1.33E-*
296 *16, FDR=1.59E-15), STK33 (p=4.6E-7, FDR=1.79E-6)* and *ERCC6L2 (p=4.57E-5,*

297 *FDR=0.00012)* (Figure 5F). These findings are extremely provocative, given that the
298 downregulated genes, particularly MYCN play a role in neuroblastomas and in several other
299 cancers.

300 We tested diacetyl for the ability to inhibit proliferation of a SH-SY5Y
301 neuroblastoma cell line from a metastatic bone tumor. A significant reduction in cell count was
302 seen in diacetyl treatments in the SH-SY5Y cancer cell lines (Figure 5G). To validate the initial
303 result, we retested diacetyl with at two concentrations across 3 different cancer cell lines. Diacetyl
304 showed a significant reduction in cell numbers for the neuroblastoma cell line specifically, and not
305 any other cell lines, relative to the control (Figure 5G). These results demonstrate that the effect is
306 specific to the SH-SY5Y cancer cell line, and unlikely to be caused by a non-specific general toxic
307 effect. It also suggests that the potential epigenetic regulation of cancer promoting genes may be
308 caused by exposure to volatiles like diacetyl in the environment.

309 **Testing therapeutic effect in neuroblastoma and Huntington's neurodegeneration**

310 Since diacetyl can affect changes in a mammalian brain by crossing the blood brain barrier,
311 we wanted to test if it can impart therapeutic effects in disorders of the brain like neurodegeneration
312 for which HDAC inhibitors have been proposed as therapeutics. In order to test diacetyl in the
313 context of neurodegenerative disease, we used the well-established *Drosophila* model of
314 Huntington's disease, which has previously been used to demonstrate the efficacy of sodium
315 butyrate in slowing neurodegeneration (27, 33). The human Huntingtin protein with expanded
316 poly-Q repeats is expressed in the neurons of the compound eye in *Drosophila*, causing progressive
317 degeneration of the seven visible photoreceptor rhabdomere cells in each ommatidium (34). We
318 selected this model in particular since polyglutamine disorders are well suited for targeting by

319 inhibitors of HDAC1 and HDAC3 (35) such as diacetyl (Figure 1B). Moreover, previous studies
320 have shown that orally administered HDAC inhibitors such as sodium butyrate and SAHA can
321 significantly reduce photoreceptor degeneration in this model (27). When the transgenic flies
322 expressing two copies of the human Huntingtin with poly-Q repeats (HTTQ120) under control of
323 the eye-specific GMR promoter were raised at 18°C, the number of rhabdomeres in each
324 ommatidium was similar to that normally observed in wild-type flies immediately post-eclosion
325 (day 1, Figures 6A-C). When these HTTQ120 flies were moved to 25° C following eclosion
326 (Figure 6A), they showed dramatic degeneration of rhabdomeres over a period of 10 days (Figures
327 6B, D-G). The mean number of rhabdomeres was reduced from 7 to ~1 by day 10. The dose of the
328 volatile in the chamber was measured in parallel experiments by tracking volatile loss and airflow
329 (0.5 L/min) and determined to range from 260-95 ppm, an average of 125 ppm at the end of hour
330 1, tapering off to 0 ppm by hour 24. The odorant was replaced each day, leading to a dosage profile
331 that would seem like a once-a-day treatment regimen (Supplemental Figure S3A).

332 Remarkably, when the Huntingtin (HTTQ120)-expressing flies were exposed immediately
333 after eclosion to volatile headspace of 1% diacetyl (Figure 6A), they showed a substantial (~50%)
334 reduction of rhabdomere loss (Figures 6B, D-G). The majority of ommatidia retained 6-7
335 rhabdomeres at day 5 (Figures 6D and F). Even after 10 days, the majority of the ommatidia still
336 had 2-3 rhabdomeres left in the odor-exposed flies, while the solvent controls had only ~1-2
337 rhabdomeres (Figures 6E and G). These results demonstrate that exposure to volatile diacetyl in
338 air slows down the photoreceptor degeneration caused in these Huntington's disease model flies.
339 Thus, odorants like diacetyl may have potential as a prophylactic against this neurodegenerative
340 disorder. Therefore, the volatile odorant can both significantly alter gene expression from a
341 distance as well as cause a phenotypic change in the fly with a human disease gene.

342 **Discussion**

343 In this study, we discovered that eukaryotic cells could alter gene expression in response
344 to an odorant, in a manner independent of traditional neuronal activity-induced pathways.
345 Members of a conserved family of HDACs detected the concentration of diacetyl differentially.
346 Diacetyl exposure increased levels of H3K9 acetylation in the nucleus in a dose-dependent manner
347 and led to changes in gene expression. The odorant diacetyl occurs naturally and is generated from
348 the metabolism of a variety of food components, including triglycerides, sugars and amino acids
349 (5). Moreover, the chemical is produced by the activity of microorganisms such as yeasts and lactic
350 bacteria during fermentation in many foods and beverages (5). Although beyond the scope of this
351 study, the discovery that cells can alter gene expression upon prolonged exposure to a common
352 naturally occurring odorant raises important questions about the potential physiological
353 consequences of the expression changes. Given our repeated exposure to particular flavors and
354 fragrances, the findings outlined here highlight a new consideration for evaluating the safety of
355 certain volatile chemicals that can cross the cell membrane.

356 In mammals, upregulation of circulating β-hydroxybutyrate during fasting or calorie
357 restriction induces changes in the expression of a set of genes (21). The acetylation mark specificity
358 and IC_{50} of β-hydroxybutyrate is similar to that of diacetyl. Any beneficial physiological effects
359 of odor-detection at lower odor concentrations would also be countered by studies of potential
360 risks at higher concentrations. In fact, the deleterious effect of exposure to high levels to diacetyl
361 causing bronchiolitis obliterans, or "popcorn lung", and its toxicity in cultured cells is already
362 known (36). Even so it is present in several foods we eat and is on the GRAS (Generally Regarded
363 as Safe) list of Flavor and Extract Manufacturers Association (FEMA) for use as a flavoring
364 ingredient at low concentrations. While the specific mechanism of "popcorn lung" is unknown, it

365 has previously been proposed that carbonyl groups of diacetyl can react to modify amino acid side
366 chains on proteins or generate reactive dicarbonyl and reactive oxygen species, leading to
367 excessive cytokine production and inflammation (37). Our results raise the possibility that the
368 molecular mechanisms underlying this disorder could also be partially attributed to the unusually
369 high HDAC-mediated genetic response to diacetyl by cells in the lungs. Several studies using
370 rodent animal models have shown toxicity of high levels of diacetyl in the respiratory tracts
371 including the nose and lungs (38, 39). The toxic effect of higher dosages has been observed for
372 many types of HDAC inhibitors. For example, in one *Drosophila* study, feeding of a high dosage
373 of 4-phenylbutyrate reduces survival rate, while a lower dosage extends longevity (40). Another
374 concern is that one of the highest known levels of diacetyl exposure to humans is through smoking
375 cigarettes, where exposure from even a single cigarette (250-361ppm) is high (41, 42): Salem (128
376 μg/cigarette), Camel (128.1 μg/cigarette), Carlton (45.6 μg/cigarette) (42). Different types of diets
377 and lifestyle choices have been known to have effects on health and well-being due to differences
378 in balance of different health promoting ingredients, yet little is known about role of such flavors,
379 fragrances and metabolites acting on epigenetic marks and altering gene expression. Our findings
380 raise the possibility that diacetyl and structurally related odors in the environment may affect gene
381 expression directly through absorption/transport into these cells. In mammals, the epithelium-lined
382 lungs and nasal/oral pathway is directly exposed to odorants presenting an opportunity to affect
383 gene expression and physiology.

384 Eukaryotes primarily detect volatile odorants in the environment using olfactory neurons
385 that express a variety of transmembrane receptors, a family of genes that have independently
386 evolved multiple times in different phyla. Examples of these unrelated genes include: the
387 ionotropic 7-transmembrane (TM) odorant receptor *(*Or*)* family, which is insect-specific; 3-TM

388 ionotropic receptors (IRs), which are present across most arthropods; the nematode-divergent 7-
389 TM GPCRs belonging to the *str, sra, srg, srw, srz, srbc, srsx* and *srr* families; the mammalian 7-
390 TM GPCR olfactory receptor (OR) family; and the trace amine-associated receptor (TAAR) family
391 (43-47). The activation of these receptors induces neuronal action potentials, and this information
392 is conveyed to higher brain centers where olfactory perception is generated (48). This second
393 response pathway which we have discovered is much slower and has an enzymatic mechanism
394 which draws parallels with the multiple pathways in place to detect light. In the specialized cells
395 of the eye, detection of light occurs via rhodopsins (7-transmembrane GPCRs) and leads to
396 neuronal activity and behavioral responses. However, other cells, including in plants, are also able
397 to respond to changes in light intensity of certain wavelengths using the ancient, conserved
398 cryptochrome proteins that are related to photolyases (49). This suggests that vital sensory
399 modalities can be detected via multiple pathways. Our observations raise the question whether
400 HDACs represent a conserved detection mechanism for odorants like diacetyl that link odor-
401 detection to a specific gene expression response. HDAC proteins, however, are an ancient family
402 of genes that predate even histones themselves (50, 51). It is conceivable that odor detection
403 mechanisms that emerged in ancient forms may not have involved specialized transmembrane
404 receptors, or neurons, or resulted in rapid behavioral movements.

405 Our data suggests that an HDAC inhibitory odorant also affects gene expression in the lungs
406 and brain of mice, including significantly decreasing the expression level of the ACE2 receptor,
407 whose ortholog in humans is the entry receptor for the SARS-CoV-2 virus that causes COVID-19.
408 The applied impact for the future could be far-reaching, as HDACs are known to affect a wide
409 variety of pathways in eukaryotes, and inhibitors are candidates for novel inhaled therapeutics as
410 treatment of many conditions such as COVID-19, cancers, neurodegeneration and a variety of

411 infectious diseases (52-60).

412 Our studies also show that one of the volatiles is protective against the neurodegenerative
413 effects of Huntington's disease model and neuroblastoma. Exposure to diacetyl volatiles in the fly
414 model of Huntington's disease reduces cell degeneration, as has been previously observed with
415 orally administered HDAC inhibitors like sodium butyrate and SAHA in this genetic model (27).
416 Previous studies indicate that the inhibition of HDACs counter the acetyltransferase inhibitory
417 activity of the polyglutamine-domain of the Htt protein which binds to p300, P/CAF and CBP (27).

418 This newly discovered activity in this class of volatile chemicals will also allow us to
419 understand how their presence in our environment, diet and microbiome shapes the epigenetic
420 landscape in the lungs and affects inflammation and immune responses. Our approach to
421 investigate consequences in model systems allows for a foundation for future research and allow
422 identification of key molecular biomarkers that can be associated with observation of epigenetic
423 effects, toxic or not, in individuals. The public health impact of these findings can be far-reaching,
424 both from the perspective of toxicity as well as therapeutics. Investigating the health safety
425 concerns of exposure to such odorants at high doses or prolonged periods is essential to understand
426 potential for damage. Conversely, at non-toxic concentrations HDAC inhibitors can be used for
427 treatment of many debilitating conditions in the lungs such as COPD, inflammation, and COVID-
428 19 infection (61).

429 Taken together, our discovery that cells can alter gene expression in response to an odor that
430 acts as an HDAC inhibitor and reprogram gene expression, promises the pursuit of new types of
431 odor-based therapeutics already approved for human consumption as prophylactics for a myriad
432 of diseases. Simultaneously, they raise the concern of a new type of environmental agent which
433 can reprogram gene expression and have widespread effects that are yet unknown.

434
435 # METHODS
436

437 ## *Drosophila* Stocks and Manipulations

438 Fly stocks were maintained on conventional fly food under a 12-hr. light:12 hr. dark cycle at 18°C
439 or 25°C. The fly strain of *w1118* backcrossed 5 times to *Canton-S* (*wCS*) was used in all the
440 *Drosophila* transcriptome experiments. P{GMR-HTT.Q120}2.4 (Bloomington # 8533) were used
441 for neurodegeneration experiments. For imaging *Gr63a-Gal4; UAS-mcd8:GFP, Gr21a-Gal4;*
442 *UAS-mcd8:GFP* stocks were obtained as a kind gift from the Carlson lab, Yale.

443 **Odor exposure experiments for imaging**

444 Newly eclosed male wCS flies were sorted in groups of 30 into vials with standard cornmeal medium.
445 Vials were closed with two overlapping 3''x3''polypropylene mesh squares and tied with cotton twine.
446 Vials were used within 6 hours. Four vials were placed in a 1000ml Nalgene straight sided jar with a
447 10ml glass beaker with 10ml of diacetyl 10^{-2} in paraffin oil. Jars were closed for exposure periods
448 ranging from 2-6 days. In recovery experiments, vials were removed from the jars and were placed in a
449 25°C incubator for the remainder of the recovery period. Flies were anesthetized on ice, sacrificed in
450 ethanol, and then immediately put into 1X phosphate buffered saline with 0.3% triton-x (PTX). Brains or
451 antenna were put in 4% paraformaldehyde in PTX and incubated for 30min while rotating at 25°C.
452 Samples were washed 5 times in PTX, and blocked in 5% natural goat serum in PTX for 1-hr while
453 rotating at 25°C. Samples were then incubated in primary antibody with 5% goat serum in PTX, mouse-
454 nc82 (1:20) (Development Studies Hybridoma Bank, University of Iowa) and rabbit-antiGFP (1:150)
455 (Invitrogen) in PTX for 48 hours in 4°C while rotating. After washing 5 times in PTX samples were
456 incubated in secondary antibody with 5% goat serum in PTX, rabbit-anti-Alexa488 (1:400) (Invitrogen)
457 and mouse-antiAlexa568 (1:400) (Invitrogen) for 48 hours in 4°C. Samples are washed 5 times in PTX

458 and stored in 70% glycerol in PTX. Images were taken using a Ziess 510 laser scanning confocal
459 microscope, and image analysis was done using Image J software.

460 **QRT-PCR**

461 Drosophila heads (with antenna) were collected on liquid nitrogen and stored at -80°C until processing.
462 300 heads were collected for each sample, and ground on liquid nitrogen. mRNA was extracted using a
463 PolyATract kit (Promega) and was reverse transcribed using Superscript III (Invitrogen) according to the
464 manufacturer's protocol. The quality of the cDNA was assessed on a 1.5% agarose gel. cDNA was
465 added to individual reactions of SYBR green master mix (BioRad) and run on a BioRad-MyQ
466 thermocycler. The program began with a single cycle for 3-min at 95°C, followed by 40 cycles of 15-sec
467 at 95°C, 30-sec at 58°C and 30-sec at 72°C. Afterward, the PCR products were heated to 95°C for 1-min
468 and cooled to 55°C for 1-min, to measure the dissociation curves. The efficiency of each primer set was
469 first validated by constructing a standard curve and three 10x serial dilutions of first strand cDNA. For
470 each serial dilution, the CT value was plotted against the log (template dilution) and the slope and r^2 value
471 of each regression line calculated. Expression of each *Or* or *Gr* gene was assessed in triplicate.
472 Dissociation curves were used to assess the purity of the PCR reactions. *Or* and *Gr* transcript levels were
473 normalized by using the transcript levels of *ribosomal protein 49*. Expression levels were calculated using
474 the Pfaffl equation.

475 In general, primers were designed by using coding sequences close to the 3' end of the gene, and where
476 possible, primers spanned an intron.

477 Primers:

478 Gr21a F: CGATCGTCTTTCCGAATCTC

479 Gr21a R: GGCTCAGATCCACCCATAGA

480 Gr63a F: AAATGAACTCCGCCTCCTTT

481 Gr63a R: CGCAATTTCAGAGGCAAACT

482 RP49 F: CTGCCCACCGGATTCAAG

483 RP49 R: GTTTCATGCGGCGAGATCG

484 Or47a F: ATCACAGGCCACATTGAACA

485 Or47a R: TCCCCGCAGTAGCAGTAGAT

486 Or88a F: TTAAAGTGGCCTTCCTGGTG

487 Or88a R: ATGCGGCAATAAAGTTCCAC

488 Or83b F: TTCTTGGCATTCGCTTTTCT

489 Or83b R: TCCCTGGATTTGTTTGCTTC

490 **Odor Exposure Protocol for Transcriptome Analysis**

491 Flies were exposed to diacetyl (B85307, Sigma-Aldrich, St. Louis, MO) by placing them in vials
492 in a cylindrical closed container (112 mm diameter x 151 mm height) along with an odor-
493 containing glass vial. The odorant was dissolved in 5 mL paraffin oil at 1% dilution. For a given
494 exposure protocol, two groups of flies were prepared: those exposed to 1% diacetyl headspace and
495 those exposed to paraffin oil headspace alone (control flies). Adult male flies aged 1 d were
496 transferred to fly vials containing fresh medium and put into the container with the odor vial. At
497 the end of the fifth day of exposure, flies were collected, and their antennae were dissected for
498 RNA extraction. All treatments and experiments were performed at room temperature. For the
499 recovery experiment, flies were transferred to a container with a glass vial of paraffin oil after 5
500 days of diacetyl exposure. At the end of the fifth day of recovery, flies were collected, and their
501 antennae were dissected for total RNA extraction. The second and third antennal segments from

502 40-60 male flies after treatment were carefully hand-dissected from the head and collected in 1.5
503 ml microfuge tubes kept cold in liquid nitrogen. Antennae were mechanically crushed with
504 disposable RNAse-free plastic pestles, and total RNA was isolated using a Trizol-based protocol.
505 cDNA libraries were prepared from total RNA using the Illumina TruSeq RNA Sample
506 Preparation Kit (v2) and 50 bps single- and paired-end sequencing was done using the
507 HighSeq2000. Two biological replicates were sequenced for each condition, with an average of
508 27 million reads / replicate, and with an average of 84% mapped.

509 Two-month-old C57BL/6 male mice (2-3 for each condition in a single cage) were
510 continually exposed to air flowing over headspace of paraffin oil (solvent control), 0.1%, or 1%
511 diacetyl over a period of 5 days, then euthanized for collecting the lung and brain tissues and
512 processing for mRNA isolation. All protocols for animal use and euthanasia were approved by the
513 Institutional Animal Care and Use Committee (#20150028) and were in accordance with the
514 provisions established by the Animal Welfare Act and the Public Health Services (PHS) Policy.
515 In the transcriptome analysis, two replicates were performed for each condition, with an average
516 of 123,687,411 reads / replicate, with an average of 88% mapped. Multiplexed libraries were
517 made from total RNA input using the Illumina TruSeq RNA sample preparation kit (v2) and 50
518 bps single-end sequencing was done using the NextSeq500.

519 **Calculation ppm in air based on weight loss of odorant over time**

520 The odor solution in PO in each setup (Drosophila and mouse) was weighed using a sensitive
521 balance. PO is non-volatile and therefore weight loss is attributable to diacetyl volatilization.
522 Volatile Headspace exposure (ppm) is calculated through odor cartridge weight change from pure
523 odor compound volatizing out (Inamdar et al., 2012).

524 $ppm=(10^6\ w/MW)/(v/V_m)$

525 Where ppm is the concentration of tested VOC in parts per million (v/v); w is the weight of the
526 tested chemical in grams; MW is the molecular weight of the tested VOC (grams/mole); v is the
527 total volume of the respective exposure chambers; and Vm is the molecular volume under the
528 tested condition.

529 •$V_m=24.45(760/P)((t+273.15)/298.15)$

530 Where 24.45 = gram molecular volume, under standard Lab conditions of 760 mm Hg, 25°C; P =
531 ambient pressure, in mm Hg; and t = ambient temperature, in °C. Odor cartridges, consisting of
532 varying odor volume/volume dilutions, were weighed periodically under standard ambient
533 temperature and pressure. Under these conditions, the pure volatile odor compounds volatize out
534 of the odor cartridge and the evaporation rates were used for our exposure calculations. Based on
535 Ideal Gas Law and experimental conditions, ppm is calculated based on volatized odor compound
536 and experimental chamber volume based on airflow.

537 **HDAC inhibitor Treatment Protocol for Transcriptome Analysis**

538 Sodium butyrate (B5887, Sigma-Aldrich) or valproic acid (P4543, Sigma-Aldrich) were dissolved
539 in normal fly food medium at the final concentration of 10 mM. Three groups of flies were
540 prepared: those treated with one of the HDAC inhibitors and those without HDAC inhibitor
541 treatment (control flies). Adult flies aged 1 d were transferred to fly vials containing medium with
542 or without a HDAC inhibitor. At the end of the fifth day of treatment, flies were collected, and
543 their antennae were dissected for RNA extraction. All treatments and experiments were performed
544 at room temperature. Two biological replicates with 60 flies/replicate were performed for each
545 condition, with an average of 23 million reads / replicate, and with an average of 92% mapped.

546 Multiplexed libraries were made from total RNA input using the Illumina TruSeq RNA sample
547 preparation kit (v2) and 50 bps paired-end sequencing was done using the HighSeq2000.

548 **Bioinformatic analysis of RNA-seq experiments**

549 Reads aligned to the latest release of each of the genomes used (dm6 for the *Drosophila* genome,
550 GRCm38 for the *Mus Musculus* genome) and quantified with kallisto (version 0.43.1) (62) Only
551 libraries for which we obtained >75 % alignment were used for downstream analysis. Transcript
552 counts were summarized to gene-level using tximport package (version 1.4.0)(63). For any
553 instances of detected batch effects, we removed unwanted variation using RuvR in the RuvSeq
554 package (version 1.10.0)(64). Differentially expressed gene (DEG) analysis was performed with
555 the edgeR package (version 3.18.1)(65) using low count filtering (cpm >0.5) and TMM
556 normalization. Protein classification analysis was performed with PANTHER (version 13.1)(66).
557 All significance analyses of gene overlap were done using the GeneOverlap package in R package
558 (version 1.14.0). GO enrichment analysis was performed using clusterProfiler (version 3.6.0)(67).

559 **HDAC Activity Assays**

560

561 HDAC activity of class I HDACs (HDAC1, 2, 3 and 8) was measured with the fluorometric HDAC
562 Activity Assay kit: HDAC1 (10011563, Cayman Chemical, Ann Arbor, MI), HDAC2, HDAC 3,
563 and HDAC 8 (50062, 50073 and 50068, BPS Bioscience, San Diego, CA), according to the
564 manufacturer's instructions. HDAC activity of class II HDACs (HDAC4 and HDAC6) were
565 measured with the fluorometric HDAC Activity Assay kit: HDAC4, HDAC 4 (50064 and 50076,
566 BPS Bioscience, San Diego, CA), according to the manufacturer's instructions. HDAC activity in
567 these 96-well format kits are directly correlated with fluorescence produced by the enzyme and

568 substrate interaction. Each test compound was tested in duplicates, minimum. Due to interference,
569 concentrations of >30 mM were not used in the IC50 calculation. To account for any potential
570 absorbance or fluorescence contributed by the test chemicals interacting with the assay substrate,
571 all baseline background measurements of test compound + substrate control wells (everything, but
572 no HDAC enzyme) were performed and subtracted against the respective test compound wells. It
573 is fair to note that no significant changes in background fluorescence were seen with tested
574 compounds in comparison to control background fluorescence. HDAC activity was calculated
575 based on averaged maximum fluorescence from negative control wells and the averaged
576 fluorescence in test compound wells.

577 $$\frac{Fluorescence_{Negative\ control} - Fluorescence_{HDACi}}{Fluorescence_{Negative\ control}} x100\% = Remaining\ HDAC\ activity\ \%$$

578 HDAC % inhibition was directly calculated from obtained HDAC activity %.

579 **Cell Culture and Treatment**

580 Human embryonic kidney 293 (HEK293) cells were grown in 100 mm cell culture dishes with
581 Dulbecco's modified Eagle's medium (DMEM) (10-013, Corning, Manassas, VA), supplemented
582 with 10% fetal bovine serum (FBS) (26140-079, Gibco, Carlsbad, CA) at 37°C with 5% CO_2.
583 Cells that were ~80% confluent were treated with freshly prepared medium supplemented with
584 diacetyl at concentrations indicated. The cells for mock controls were handled in the same manner
585 without adding diacetyl to the medium. To prevent diffusion of diacetyl odor from the treatment
586 dishes to the ones of mock control, the cell culture dishes in different conditions were cultured in
587 separate CO_2 incubators.

588 Cell proliferation assays were performed to assess effects of compounds against cancer cell lines.
589 Cells were maintained in a 37°C incubator with 5% CO_2 throughout the whole experiment.

590 Compound stocks are dissolved in 10% DMSO, and final concentrations made fresh in complete
591 media as needed. 10% DMSO solvent is used as control in complete media. Cells were seeded
592 onto 12-well plates and allowed 12-24 hours until treatment to allow cells to adhere to wells.
593 This is followed by minimum 5-day treatment of compounds, changing the media with treatment
594 every 48 hours. Cell lines A549, PC3, and SK-MEL-5 will be seeded at 8000 cells/well, which
595 was determined to provide 80-100% confluency after 6-day growth. SH-SY5Y was seeded at
596 8000 cells/well and 16,000 cells/well due to their known slower division rate and given at least
597 10 days for sufficient growth. After allotted growth times, cell counts were performed using the
598 Countess™ automated cell counter. All assays had a minimum of three replicates for all
599 conditions and analyzed through GraphPad Prism One-way ANOVA for significance.

600 **Odor Exposure Protocol for Huntington's Disease Model Flies**

601 Flies were exposed to diacetyl in a cylindrical container (112 mm diameter x 151 mm height).
602 Each container was tightly closed but had 2 holes, one of which connected to an air suction port,
603 and the other to a vial containing either of 5 mL paraffin oil or 5 mL 1% diacetyl in paraffin oil. A
604 gentle suction was applied to pull the headspace from the odor or paraffin oil vials into the
605 cylindrical structure. pGMR-HTTQ120 flies were maintained at 18°C. Adult flies aged 1 d were
606 transferred to fly vials containing fresh medium and put into the odor-filled container at room
607 temperature. Paraffin oil and 1% diacetyl solution were prepared and replaced every day. At the
608 end of the fifth day of exposure, half of the flies were collected and subjected to pseudopupil
609 analysis as before (27). The remaining flies were transferred to fresh medium and exposed to the
610 odors for an additional 5 days. All treatments and experiments were performed at room
611 temperature. The number of rhabdomeres in each ommatidium was counted using the pseudopupil

612 analysis, and statistical significance was determined by unpaired t test (two-tailed) against PO at
613 each time point.

614 **Preparation of Nuclear Extracts from HEK293 Cells**

615 Nuclear extracts of HEK293 cells were prepared according to a protocol described previously (68),
616 with minor modifications. In brief, HEK293 cells were washed twice with cold phosphate-buffered
617 saline (PBS) and lysed with hypotonic buffer (10 mM HEPES-KOH [pH 7.9], 1.5 mM $MgCl_2$, 10
618 mM KCl, protease inhibitor cocktail (04693159001, Roche, Indianapolis, IN), 1 mM DTT, 1 mM
619 TSA). Following a brief centrifugation, the pellet was resuspended in hypertonic buffer (20 mM
620 HEPES-KOH [pH 7.9], 25% glycerol, 420 mM NaCl 1.5 mM $MgCl_2$, 0.2 mM EDTA, protease
621 inhibitor cocktail, 1 mM DTT, 1 mM TSA). The supernatant was recovered as nuclear extract.

622 **Western Blot Analysis**

623 Proteins in the nuclear extracts (60 μg protein) were separated by SDS–PAGE gels (456-1043,
624 Bio-Rad, Hercules, CA), transferred onto PVDF membranes (162-0174, Bio-Rad), and incubated
625 with anti-histone antibodies: acetylated H3K9 (1/2000: ab4441, abcam, Cambridge, MA),
626 acetylated H3K14 (1/5000: 06-911, EMD Millipore, Billerica, MA), acetylated H4K5 (1/2000:
627 07-327, EMD Millipore). Bound antibody was detected by horseradish peroxidase-conjugated
628 anti-rabbit secondary antibody (1/20000: 1705046, Bio-Rad) and developed using Clarity™
629 Western ECL Substrate (1705060, Bio-Rad). Signals were detected and captured by
630 ImageQuant™ LAS 4000 mini (GE healthcare, Pittsburgh, PA), and band intensities were
631 quantified with ImageJ software. H3K9 acetylation intensity in individual lanes was reported
632 relative to the normalized Mock treatment and calculated using this formula: Relative H3K9ace
633 intensity for each timepoint = (H3K9ace / PCNA) / averaged (Mock H3K9ace / Mock PCNA).

634 Statistical significance was determined by unpaired *t* test (two-tailed) against mock at each time
635 point.

636 **Data availability**

637 All transcriptome data sets in this publication have been deposited in the GEO repository
638 with accession number GSE116502. All other data is presented in the figures, tables, and
639 supplementary materials.

640 **Author contributions:** S. H.Y. performed the biochemical assays, cell culture assays,
641 neurodegeneration assays and wrote the first draft. R.N.F performed biochemical assays and the
642 cancer cell line exposure experiments and helped write the paper. C.A.S performed the
643 bioinformatics and transcriptome analysis, parts of the biochemical assays, and helped write the
644 paper. S.P. performed some of the transcriptome analysis. S.T.C performed the imaging studies
645 and RT-PCR. C.P. performed some biochemical analyses. M.G.N. helped plan and assisted with
646 the mouse exposure experiments. A.R. conceptualized the study, planned, and supervised the
647 experiments and wrote the final draft of the paper.

648 **Competing interests:** A.R. is founder of startups: Sensorygen working on computational
649 neurobiology of olfaction and taste, and Remote Epigenetics working on small molecule
650 enhancement of agricultural production. A.R., S.T.C., S.H.Y., R.N-F., are listed as inventors on
651 patents filed by University of California.

652 **Acknowledgments:** We would like to thank Dr. Larry Marsh for advice about the fly eye assay
653 and HDAC inhibitors, Joel Kowalewski for help with critical comments, Dr. Thomas Girke for
654 guidance in bioinformatics analysis, Drs. Anupama Dahanukar, Naoki Yamanaka, Chih-cheng
655 Tsai, Karine LeRoch and Adler R. Dillman for sharing equipment and reagents. This work was

partially supported by funds provided by the National Institutes of Health, NIAID (R01AI153195 to M.G.N and R01AI087785 to A.R), and HATCH funds from the Agricultural Experimentation Station UC Riverside to A.R.

References

1. McFall-Ngai M*, et al.* (2013) Animals in a bacterial world, a new imperative for the life sciences. *Proceedings of the National Academy of Sciences* 110(9):3229-3236 %U http://www.pnas.org/content/3110/3229/3229.
2. Dorrestein PC, Mazmanian SK, & Knight R (2014) Finding the missing links among metabolites, microbes, and the host. *Immunity* 40(6):824-832.
3. Wikoff WR*, et al.* (2009) Metabolomics analysis reveals large effects of gut microflora on mammalian blood metabolites. *Proceedings of the National Academy of Sciences* 106(10):3698-3703 %U http://www.pnas.org/content/3106/3610/3698.
4. Rooks MG & Garrett WS (2016) Gut microbiota, metabolites and host immunity. *Nat Rev Immunol* 16(6):341-352.
5. Shibamoto T (2014) Diacetyl: occurrence, analysis, and toxicity. *J Agric Food Chem* 62(18):4048-4053.
6. Devaud JM, Acebes A, & Ferrus A (2001) Odor exposure causes central adaptation and morphological changes in selected olfactory glomeruli in Drosophila. *Journal of Neuroscience* 21(16):6274-6282.
7. Sachse S*, et al.* (2007) Activity-dependent plasticity in an olfactory circuit. *Neuron* 56(5):838-850.
8. Devaud JM, Acebes A, & Ferrus A (2001) Odor exposure causes central adaptation and morphological changes in selected olfactory glomeruli in Drosophila. *J Neurosci* 21(16):6274-6282.
9. Martineau B, Henick-Kling, T., Acree, T. (1995) Reassessment of the Influence of Malolactic Fermentation on the Concentration of Diacetyl in Wines. *Am J Enol Vitic* 46(3):385-388.
10. Nykanen L, Nykanen, I. (1991) Distilled beverages. *Volatile Compounds in Foods and Beverages*, ed Maarse H (Dekker Inc, New York), pp 548-580.
11. Hughes PS, Baxter, E.D. (2001) Flavour Determinants of Beer Quality. *Beer: Quality, Safety and Nutritional Aspects*, (The Royal Society od Chemistry, Camdridge, UK), pp 40-73.
12. Turner SL & Ray A (2009) Modification of CO2 avoidance behaviour in Drosophila by inhibitory odorants. *Nature* 461(7261):277-281.
13. Shahbazian MD & Grunstein M (2007) Functions of site-specific histone acetylation and deacetylation. *Annu Rev Biochem* 76:75-100.
14. Graff J & Tsai LH (2013) Histone acetylation: molecular mnemonics on the chromatin. *Nat Rev Neurosci* 14(2):97-111.
15. Minucci S & Pelicci PG (2006) Histone deacetylase inhibitors and the promise of epigenetic (and more) treatments for cancer. *Nat Rev Cancer* 6(1):38-51.
16. Kazantsev AG & Thompson LM (2008) Therapeutic application of histone deacetylase inhibitors for central nervous system disorders. *Nat Rev Drug Discov* 7(10):854-868.
17. Chuang DM, Leng Y, Marinova Z, Kim HJ, & Chiu CT (2009) Multiple roles of HDAC inhibition in neurodegenerative conditions. *Trends Neurosci* 32(11):591-601.
18. Jones WD, Cayirlioglu P, Kadow IG, & Vosshall LB (2007) Two chemosensory receptors together mediate carbon dioxide detection in Drosophila. *Nature* 445:86-90.
19. Berdnik D, Chihara T, Couto A, & Luo L (2006) Wiring Stability of the Adult Drosophila Olfactory Circuit after Lesion. *J. Neurosci.* 26(13):3367-3376.

20. Sigg D, Thompson CM, & Mercer AR (1997) Activity-Dependent Changes to the Brain and Behavior of the Honey Bee, Apis mellifera (L.). *J. Neurosci.* 17(18):7148-7156.
21. Shimazu T*, et al.* (2013) Suppression of oxidative stress by beta-hydroxybutyrate, an endogenous histone deacetylase inhibitor. *Science* 339(6116):211-214.
22. Whiteson KL*, et al.* (2014) Breath gas metabolites and bacterial metagenomes from cystic fibrosis airways indicate active pH neutral 2,3-butanedione fermentation. *ISME J* 8(6):1247-1258.
23. Krogerus K & Gibson BR (2013) Influence of valine and other amino acids on total diacetyl and 2,3-pentanedione levels during fermentation of brewer's wort. *Appl Microbiol Biotechnol* 97(15):6919-6930.
24. Krautkramer KA, Rey FE, & JM. D (2017) Chemical signaling between gut microbiota and host chromatin: What is your gut really saying? . *J Biol Chem* 292(21):8582-8593.
25. James A, Austin C, Cox D, Taylor D, & Calvert R (2013) Microbiological and biochemical origins of human axillary odour. *FEMS Microbiol Ecol* 83(3):527-540.
26. Effantin G, Rivasseau C, Gromova M, Bligny R, & Hugouvieux-Cotte-Pattat N (2011) Massive production of butanediol during plant infection by phytopathogenic bacteria of the genera Dickeya and Pectobacterium. *Molecular microbiology* 82(4):988-997.
27. Steffan JS*, et al.* (2001) Histone deacetylase inhibitors arrest polyglutamine-dependent neurodegeneration in Drosophila. *Nature* 413(6857):739-743.
28. Fischer A (2010) [HDAC inhibitors as therapy for neural disorders. Discovery of a new therapy]. *Pharm Unserer Zeit* 39(3):204-209.
29. Chauhan MB & Chauhan NB (2015) Brain Uptake of Neurotherapeutics after Intranasal versus Intraperitoneal Delivery in Mice. *J Neurol Neurosurg* 2(1).
30. Jansky S*, et al.* (2021) Single-cell transcriptomic analyses provide insights into the developmental origins of neuroblastoma. *Nature Genetics* 53(5):683-693.
31. Pugh TJ*, et al.* (2013) The genetic landscape of high-risk neuroblastoma. *Nature Genetics* 45(3):279-284.
32. Zhong X*, et al.* (2018) Identification of Potential Prognostic Genes for Neuroblastoma. *Front Genet* 9.
33. Marsh JL & Thompson LM (2006) Drosophila in the study of neurodegenerative disease. *Neuron* 52(1):169-178.
34. Jackson GR*, et al.* (1998) Polyglutamine-expanded human huntingtin transgenes induce degeneration of Drosophila photoreceptor neurons. *Neuron* 21(3):633-642.
35. Thomas EA (2014) Involvement of HDAC1 and HDAC3 in the Pathology of Polyglutamine Disorders: Therapeutic Implications for Selective HDAC1/HDAC3 Inhibitors. *Pharmaceuticals (Basel)* 7(6):634-661.
36. More SS, Raza A, & Vince R (2012) The butter flavorant, diacetyl, forms a covalent adduct with 2-deoxyguanosine, uncoils DNA, and leads to cell death. *J Agric Food Chem* 60(12):3311-3317.
37. Starek-Swiechowicz B & Starek A (2014) Diacetyl exposure as a pneumotoxic factor: a review. *Rocz Panstw Zakl Hig* 65(2):87-92.
38. Morgan DL, Flake GP, Kirby PJ, & Palmer SM (2008) Respiratory toxicity of diacetyl in C57BL/6 mice. *Toxicol Sci* 103(1):169-180.
39. Palmer SM*, et al.* (2011) Severe airway epithelial injury, aberrant repair and bronchiolitis obliterans develops after diacetyl instillation in rats. *PLoS One* 6(3):e17644.
40. Kang HL, Benzer S, & Min KT (2002) Life extension in Drosophila by feeding a drug. *Proc Natl Acad Sci U S A* 99(2):838-843.
41. Rigler MW & Longo WE (2010) Emission of diacetyl (2,3 butanedione) from natural butter, microwave popcorn butter flavor powder, paste, and liquid products. *Int J Occup Environ Health* 16(3):291-302.
42. Pierce JS, Abelmann A, Spicer LJ, Adams RE, & Finley BL (2014) Diacetyl and 2,3-pentanedione exposures associated with cigarette smoking: implications for risk assessment of food and flavoring workers. *Crit Rev Toxicol* 44(5):420-435.

753 43. Buck L & Axel R (1991) A Novel Multigene Family May Encode Odorant Receptors: A
754 Molecular Basis for Odor Recognition. *Cell* 65:175-187.
755 44. Clyne PJ*, et al.* (1999) A novel family of divergent seven-transmembrane proteins: candidate
756 odorant receptors in *Drosophila*. *Neuron* 22(2):327-338.
757 45. Troemel ER, Chou JH, Dwyer ND, Colbert HA, & Bargmann CI (1995) Divergent seven
758 transmembrane receptors are candidate chemosensory receptors in *C. elegans*. *Cell* 83(2):207-
759 218.
760 46. Benton R, Vannice K, Gomezdiaz C, & Vosshall L (2009) Variant Ionotropic Glutamate
761 Receptors as Chemosensory Receptors in Drosophila. *Cell* 136(1):149-162.
762 47. Vosshall LB, Amrein H, Morozov PS, Rzhetsky A, & Axel R (1999) A spatial map of olfactory
763 receptor expression in the *Drosophila* antenna. *Cell* 96(5):725-736.
764 48. Knaden M & Hansson BS (2014) Mapping odor valence in the brain of flies and mice. *Curr Opin*
765 *Neurobiol* 24(1):34-38.
766 49. Fogle KJ*, et al.* (2015) CRYPTOCHROME-mediated phototransduction by modulation of the
767 potassium ion channel beta-subunit redox sensor. *Proc Natl Acad Sci U S A* 112(7):2245-2250.
768 50. Gregoretti IV, Lee YM, & Goodson HV (2004) Molecular evolution of the histone deacetylase
769 family: functional implications of phylogenetic analysis. *J Mol Biol* 338(1):17-31.
770 51. Postberg J, Forcob S, Chang WJ, & Lipps HJ (2010) The evolutionary history of histone H3
771 suggests a deep eukaryotic root of chromatin modifying mechanisms. *BMC Evol Biol* 10:259.
772 52. Witt O & Lindemann R (2009) HDAC inhibitors: magic bullets, dirty drugs or just another
773 targeted therapy. *Cancer Lett* 280(2):123-124.
774 53. Wang J*, et al.* (2013) Potential advantages of CUDC-101, a multitargeted HDAC, EGFR, and
775 HER2 inhibitor, in treating drug resistance and preventing cancer cell migration and invasion.
776 *Mol Cancer Ther* 12(6):925-936.
777 54. Wang J*, et al.* (2012) Sirtinol, a class III HDAC inhibitor, induces apoptotic and autophagic cell
778 death in MCF-7 human breast cancer cells. *Int J Oncol* 41(3):1101-1109.
779 55. Yeung A*, et al.* (2012) HDAC inhibitor M344 suppresses MCF-7 breast cancer cell proliferation.
780 *Biomed Pharmacother* 66(3):232-236.
781 56. Park JH*, et al.* (2012) A new synthetic HDAC inhibitor, MHY218, induces apoptosis or
782 autophagy-related cell death in tamoxifen-resistant MCF-7 breast cancer cells. *Invest New Drugs*
783 30(5):1887-1898.
784 57. Cai X*, et al.* (2010) Discovery of 7-(4-(3-ethynylphenylamino)-7-methoxyquinazolin-6-yloxy)-N-
785 hydroxyheptanamide (CUDc-101) as a potent multi-acting HDAC, EGFR, and HER2 inhibitor
786 for the treatment of cancer. *J Med Chem* 53(5):2000-2009.
787 58. Shankar S & Srivastava RK (2008) Histone deacetylase inhibitors: mechanisms and clinical
788 significance in cancer: HDAC inhibitor-induced apoptosis. *Adv Exp Med Biol* 615:261-298.
789 59. Platta CS, Greenblatt DY, Kunnimalaiyaan M, & Chen H (2007) The HDAC inhibitor trichostatin
790 A inhibits growth of small cell lung cancer cells. *J Surg Res* 142(2):219-226.
791 60. Komatsu N*, et al.* (2006) SAHA, a HDAC inhibitor, has profound anti-growth activity against
792 non-small cell lung cancer cells. *Oncol Rep* 15(1):187-191.
793 61. Shakespear MR, Halili MA, Irvine KM, Fairlie DP, & Sweet MJ (2011) Histone deacetylases as
794 regulators of inflammation and immunity. *Trends Immunol* 32(7):335-343.
795 62. Bray NL, Pimentel H, Melsted P, & Pachter L (2016) Near-optimal probabilistic RNA-seq
796 quantification. *Nat Biotechnol* 34(5):525-527.
797 63. Soneson C, Love MI, & Robinson MD (2015) Differential analyses for RNA-seq: transcript-level
798 estimates improve gene-level inferences. *F1000Res* 4:1521.
799 64. Risso D, Ngai J, Speed TP, & Dudoit S (2014) Normalization of RNA-seq data using factor
800 analysis of control genes or samples. *Nat Biotechnol* 32(9):896-902.
801 65. Robinson MD, McCarthy DJ, & Smyth GK (2010) edgeR: a Bioconductor package for
802 differential expression analysis of digital gene expression data. *Bioinformatics* 26(1):139-140.

803 66. Mi H, *et al.* (2017) PANTHER version 11: expanded annotation data from Gene Ontology and
804 Reactome pathways, and data analysis tool enhancements. *Nucleic Acids Res* 45(D1):D183-D189.
805 67. Yu G, Wang LG, Han Y, & He QY (2012) clusterProfiler: an R package for comparing biological
806 themes among gene clusters. *OMICS* 16(5):284-287.
807 68. Andrews NC & Faller DV (1991) A rapid micropreparation technique for extraction of DNA-
808 binding proteins from limiting numbers of mammalian cells. *Nucleic Acids Res* 19(9):2499.

809

810

811 # Figure Legends

812 **Figure 1. Volatiles found in microbes can inhibit HDACs in vitro**

813 (**A**) Antennal and whole mount brain staining of *Gr63a-Gal4* flies. Flies were exposed to diacetyl
814 (headspace from 10^{-2} soln) or air for 2 to 5 days. Brains and antenna were dissected on the
815 indicated days, fixed, and then stained for neuropil marker nc82 (red) and anti-GFP (green). (**B)**
816 Mean of ab1C neurons expressing GFP after indicated days of odor exposure. d4on=2,3-
817 butanedione. n=6, error bars=s.e.m. Schematic chemical structures of diacetyl, β-hydroxybutyrate
818 and Sodium butyrate. **(C)** Dose-activity curves of class I HDACs: HDAC1, HDAC2, HDAC3,
819 HDAC8 and class II HDAC6 treated with various concentrations of diacetyl. Percentage of HDAC
820 activity is relative to the activity of each enzyme without diacetyl. IC50s are indicated in the chart
821 areas. Error bars, S.E.M., n = 4-5. **(E)** Representative structures of odorants that inhibit HDACs,
822 and **(F)** Average percentage inhibition of class I HDACs: HDAC1, HDAC3 and class II HDAC4,
823 HDAC6 treated with 15mM of indicated volatiles. Error bar= S.D., each tested in duplicate.

824 **Figure 2. Diacetyl increases level of histone acetylation in HEK293 cells**

825 **(A and B)** Representative images from Western blots showing acetylation levels of H3K9 (left),
826 H3K14 (middle) and H4K5 (right) in HEK293 cells after 2 hours **(A)** and 6 hours **(B)** of diacetyl
827 exposure. PCNA (Proliferating cell nuclear antigen) is a 29 kDa nuclear protein used as a loading
828 control for nuclear protein extracts. **(C)** Western blots showing acetylation levels of H3K9 in
829 HEK293 cells treated with 100 μM diacetyl for 72, 96, and120 hours. PCNA is used for a loading
830 control. **(D)** Bar graph showing the relative intensities of acetylated H3K9 in HEK293 cells treated
831 with 100 μM diacetyl for 72 -120 hours. n = 4 samples, * $p < 0.05$, and **** $p < 0.0001$.

832 **Figure 3. Remote exposure to HDACi volatile alters gene expression in an invertebrate, and**
833 **vertebrate.**

834 (**A**) Schematic of odor exposure protocol for transcriptome analysis from the antennae. (**B**) Plot
835 highlighting up- and down-regulated genes in the diacetyl-exposed group. Red and blue dots
836 represent up-regulated genes (false discovery rate (FDR) < 0.05, $\log_2$ fold change (LFC) > 1) and
837 down-regulated genes (FDR < 0.05, LFC < 1), respectively. (**C**) Bar graphs denoting the protein
838 classification of the genes up- and down-regulated after odor exposure. **(D)** Schematic of diacetyl
839 exposure protocol for transcriptome analysis of mouse lung tissue. **(E)** Plot highlighting up- and
840 down-regulated genes in the diacetyl-exposed groups. Red and blue dots represent up-regulated
841 genes (FDR < 0.05, LFC > 1) and down-regulated genes (FDR < 0.05, LFC < 1), respectively in
842 lungs. **(F)** Table showing pairwise tests of significance of overlap between gene sets. P-values
843 from Fisher's exact test, colored with associated odds ratio (strength of association). **(G and H)**
844 Bar graphs denoting the protein classification of the genes up- and down-regulated in the lung after
845 exposure to headspace above 0.1% (v/v) **(G)** and 1% (v/v) **(H)** of diacetyl solutions.

846 **Figure 4. Gene expression changes are partly reversible, and overlaps with known HDACi**
847 **drugs**

848 (**A**) Schematic of odor exposure and recovery protocol for transcriptome analysis from the
849 antennae. (**B**) Plot highlighting up- and down-regulated genes in the recovery from diacetyl
850 exposure group. Red and blue dots represent up-regulated genes (FDR < 0.05, LFC > 1) and down-
851 regulated genes (FDR < 0.05, LFC < 1), respectively. (**C**) Table showing pairwise tests of
852 significance of overlap between gene sets. P-values from Fisher's exact test, colored with
853 associated odds ratio (strength of association). (**D** and **E**) Plots showing enrichment of up- and

854 down-regulated genes in sodium butyrate- (**D**) and valproic acid-treated (**E**) groups. Red and blue
855 dots represent up-regulated genes (FDR < 0.05, LFC > 1) and down-regulated genes (FDR < 0.05,
856 LFC < 1), respectively. (**F**) *Left:* Venn diagrams showing the overlaps of up-regulated genes
857 among diacetyl-, sodium butyrate- and valproic acid-treated groups. *Right:* Table showing
858 pairwise tests of significance of overlap between gene sets. P-values from Fisher's exact test. (**G**
859 **and H)** GO-enrichment analysis of the common Up-regulated and down-regulated genes across
860 all 3 treatments in (**F**)**.**

861 **Figure 5. Exposure to diacetyl vapor alters gene expression in the mouse brain**

862 **(A)** Schematic of diacetyl exposure protocol for transcriptome analysis of mouse brain tissues. **(B**
863 **and C)** Plot showing up- and down-regulated genes in the diacetyl-exposed groups. Red and blue
864 dots represent up-regulated genes (FDR < 0.05, LFC > 1) and down-regulated genes (FDR < 0.05,
865 LFC < 1), respectively in the brain. **(D)** *Left:* Table showing pairwise tests of significance of
866 overlap between gene sets. P-values from Fisher's exact test. *Right:* Venn diagrams showing the
867 overlaps of DEGs between lung and brain groups. **(E)** Bar graphs denoting the protein
868 classification of the brain genes up- and down-regulated after 1% diacetyl exposure. **(F)** Mean fold
869 change of select neuroblastoma related genes in the brain of mice exposed to diacetyl vapors. **(G)**
870 Cell counts of indicated cancer cell lines in tissue culture treated with solvent control or indicated
871 concentration of diacetyl. N=3-6, p<0.001.

872 **Figure 6. Odor exposure slows Huntington's neurodegeneration model in fly eye**

873 **(A)** Schematic diagram showing temperature of experimental condition and timing of the eye
874 examination in pGMR-HTTQ120 flies. **(B)** Bar graph showing mean number of rhabdomeres in
875 each ommatidium in solvent paraffin oil (PO, blue) and diacetyl-exposed (red) pGMR-HTTQ120

876 flies at 1, 5, and 10 days after eclosion (AE). n = 600 ommatidia from 15 flies, **** $p < 0.0001$.
877 **(C)** A representative image of ommatidia of pGMR-HTTQ120 flies at 1 day AE. **(D and E)**
878 Representative images of ommatidia of pGMR-HTTQ120 flies exposed to paraffin oil (PO) or
879 diacetyl at 5 **(D)** and 10 **(E)** days AE. **(F and G)** Histogram showing the percent of the ommatidium
880 with a given number of rhabdomeres indicated on the x axis at 5 **(F)** and 10 **(G)** days AE.

881

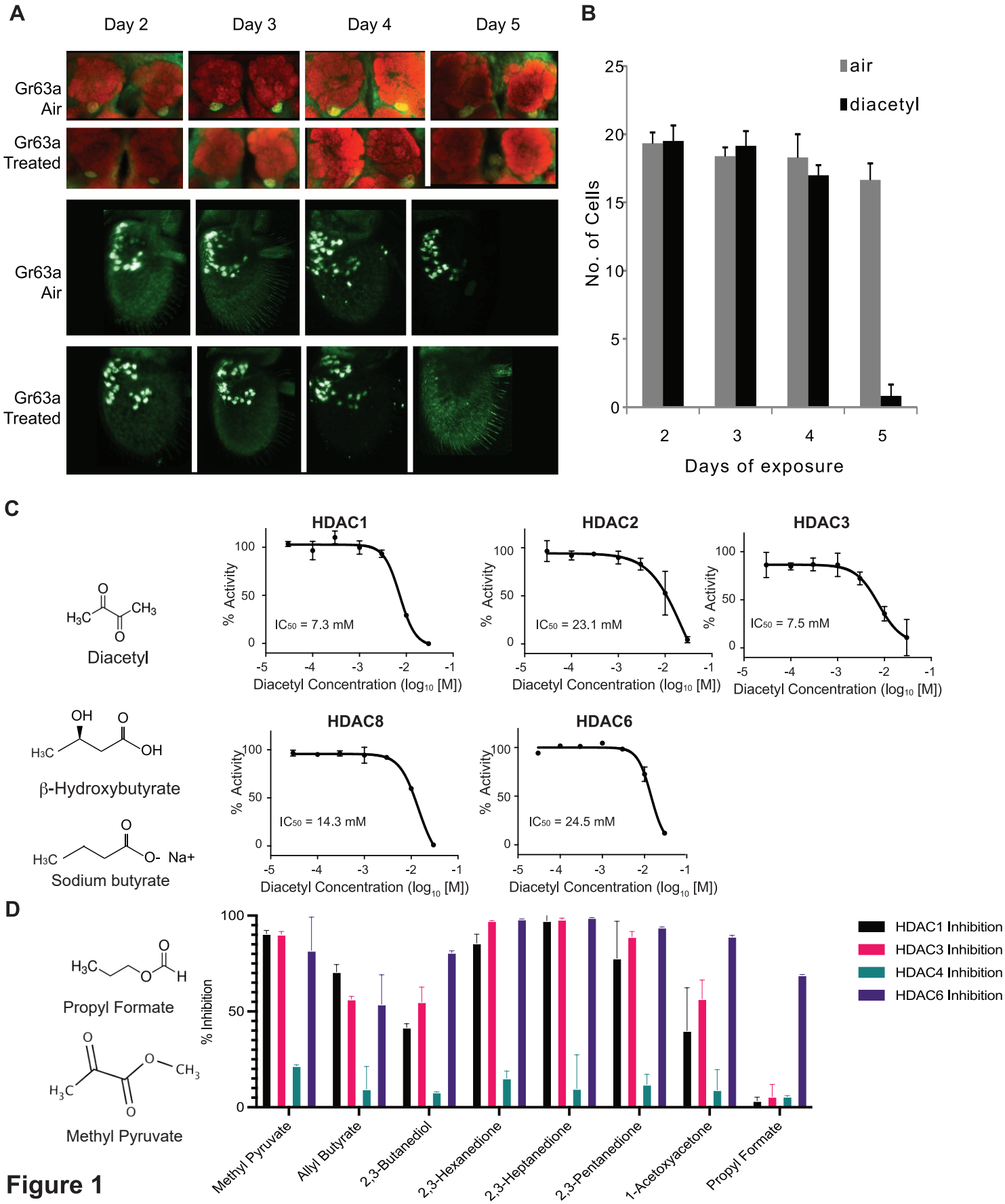
A
Day 2
Day 3
Day 4
Day 5
Gr63a Air
Gr63a Treated
Gr63a Air
Gr63a Treated
B
air
diacetyl
No. of Cells
Days of exposure
C
Diacetyl
β-Hydroxybutyrate
Sodium butyrate
HDAC1
HDAC2
HDAC3
HDAC8
HDAC6
% Activity
IC50 = 7.3 mM
IC50 = 23.1 mM
IC50 = 7.5 mM
IC50 = 14.3 mM
IC50 = 24.5 mM
Diacetyl Concentration (log10 [M])
D
Propyl Formate
Methyl Pyruvate
% Inhibition
HDAC1 Inhibition
HDAC3 Inhibition
HDAC4 Inhibition
HDAC6 Inhibition
Methyl Pyruvate
Allyl Butyrate
2,3-Butanediol
2,3-Hexanedione
2,3-Heptanedione
2,3-Pentanedione
1-Acetoxyacetone
Propyl Formate

Figure 1

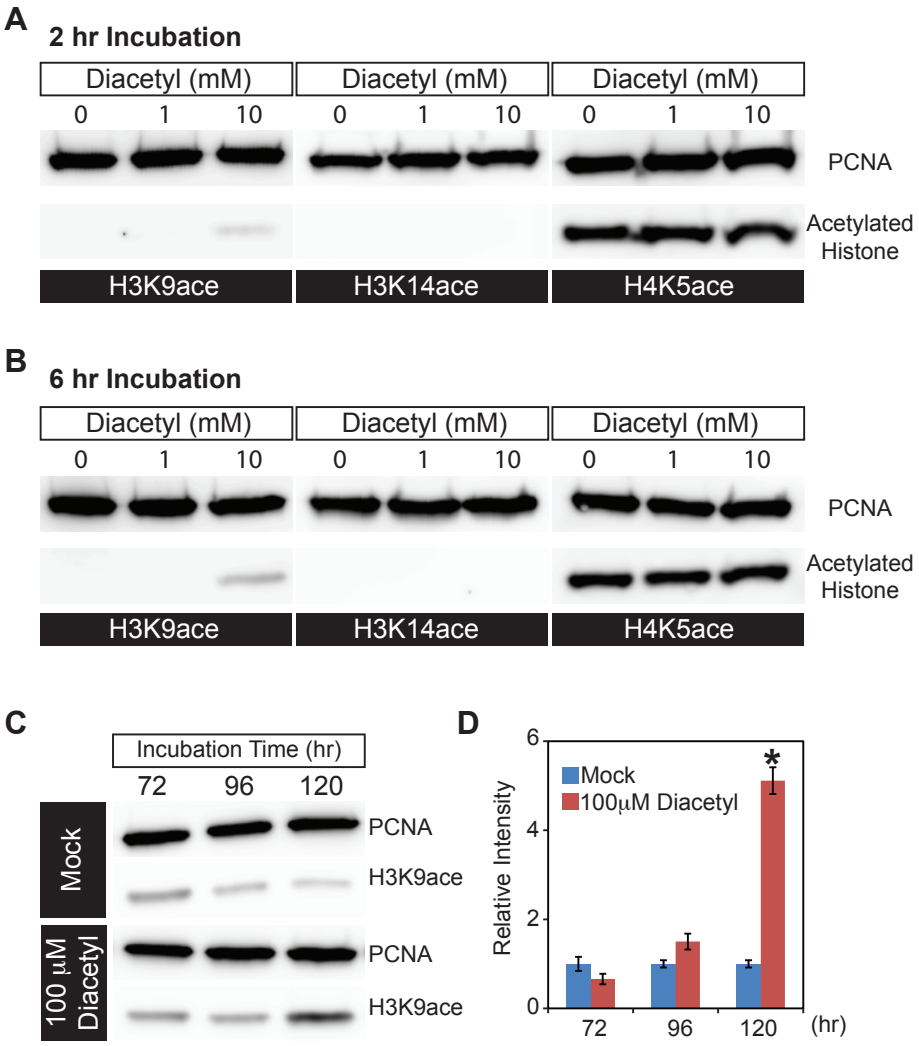
A
2 hr Incubation
Diacetyl (mM)
0 1 10
PCNA
Acetylated Histone
H3K9ace
H3K14ace
H4K5ace
B
6 hr Incubation
C
Incubation Time (hr)
72 96 120
Mock
100 μM Diacetyl
D
Mock
100μM Diacetyl
Relative Intensity
(hr)

Figure 2

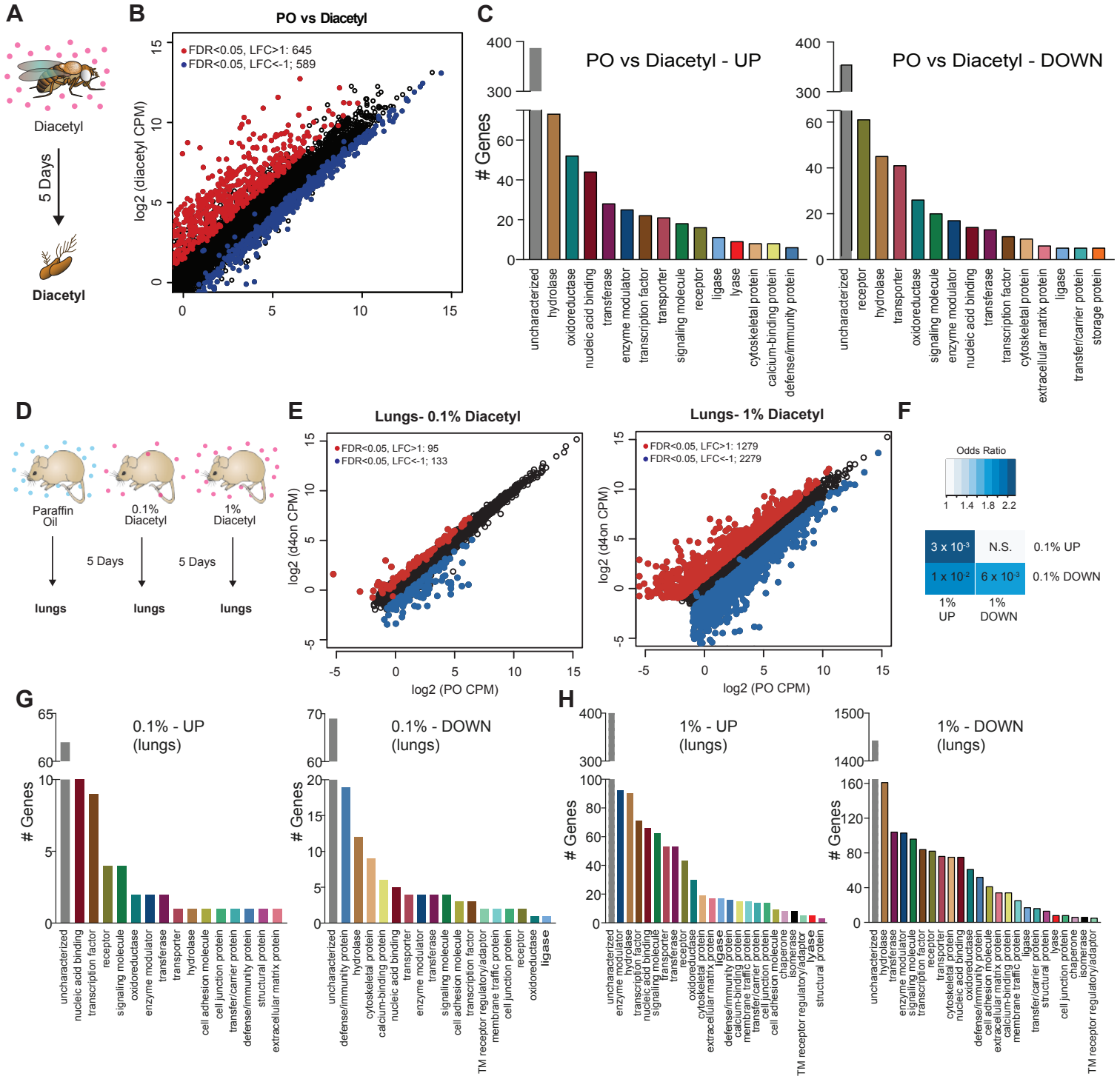
A
Diacetyl
5 Days
Diacetyl
B
PO vs Diacetyl
FDR<0.05, LFC>1: 645
FDR<0.05, LFC<-1; 589
log2 (diacetyl CPM)
C
PO vs Diacetyl - UP
PO vs Diacetyl - DOWN
Genes
uncharacterized
hydrolase
oxidoreductase
nucleic acid binding
transferase
enzyme modulator
transcription factor
transporter
signaling molecule
receptor
ligase
lyase
cytoskeletal protein
calcium-binding protein
defense/immunity protein
extracellular matrix protein
storage protein
transfer/carrier protein
D
Paraffin Oil
0.1% Diacetyl
1% Diacetyl
5 Days
5 Days
lungs
lungs
lungs
E
Lungs- 0.1% Diacetyl
FDR<0.05, LFC>1: 95
FDR<0.05, LFC<-1; 133
Lungs- 1% Diacetyl
FDR<0.05, LFC>1: 1279
FDR<0.05, LFC<-1; 2279
log2 (d4on CPM)
log2 (PO CPM)
F
Odds Ratio
1 1.4 1.8 2.2
3 x 10-3
N.S.
0.1% UP
1 x 10-2
6 x 10-3
0.1% DOWN
1% UP
1% DOWN
G
0.1% - UP (lungs)
0.1% - DOWN (lungs)
H
1% - UP (lungs)
1% - DOWN (lungs)
Genes

Figure 3

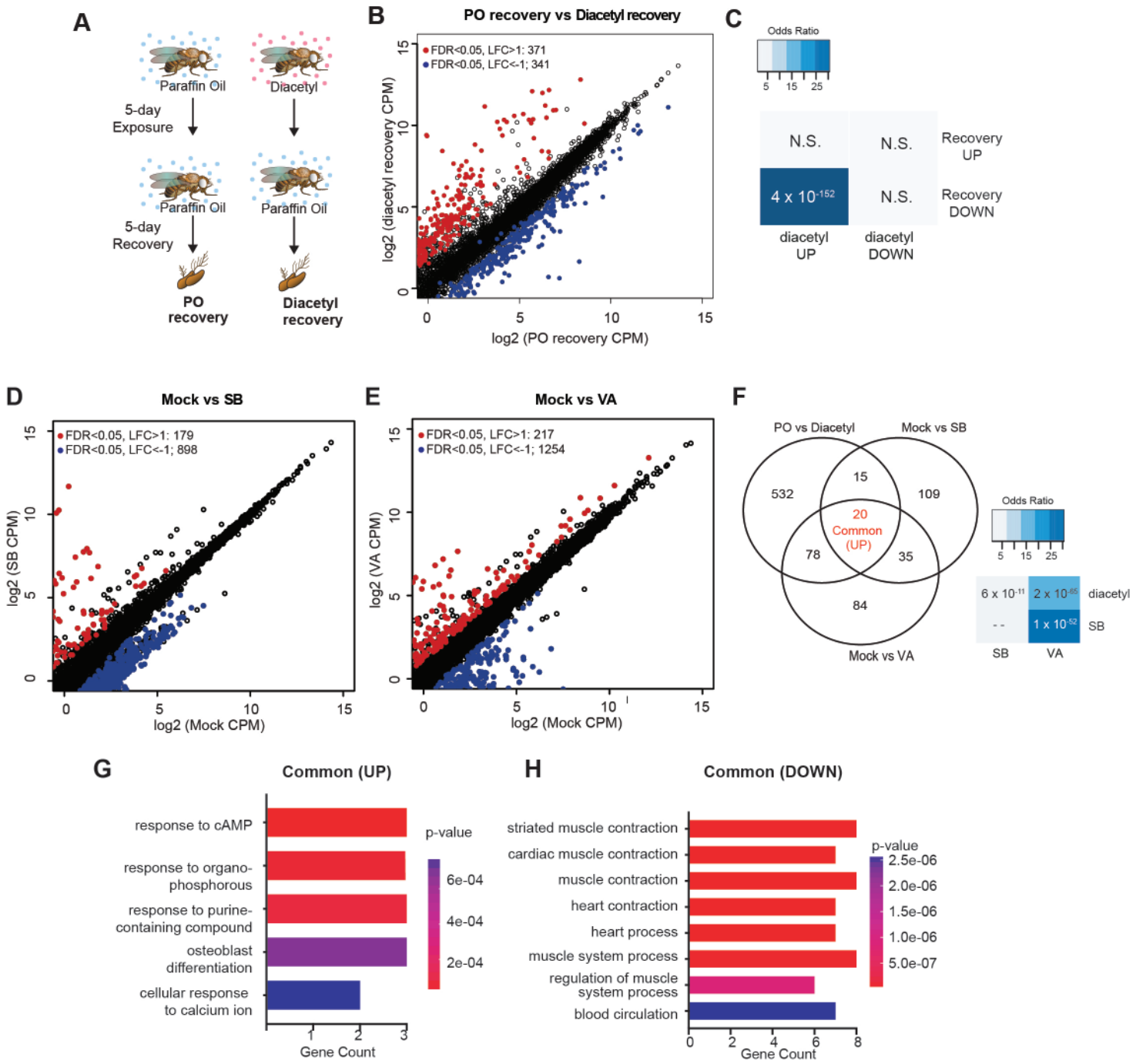
A
Paraffin Oil
Diacetyl
5-day Exposure
Paraffin Oil
Paraffin Oil
5-day Recovery
PO recovery
Diacetyl recovery
B
PO recovery vs Diacetyl recovery
FDR<0.05, LFC>1: 371
FDR<0.05, LFC<-1; 341
log2 (diacetyl recovery CPM)
log2 (PO recovery CPM)
C
Odds Ratio
5 15 25
N.S.
N.S.
Recovery UP
4 x 10-152
N.S.
Recovery DOWN
diacetyl UP
diacetyl DOWN
D
Mock vs SB
FDR<0.05, LFC>1: 179
FDR<0.05, LFC<-1; 898
log2 (SB CPM)
log2 (Mock CPM)
E
Mock vs VA
FDR<0.05, LFC>1: 217
FDR<0.05, LFC<-1; 1254
log2 (VA CPM)
log2 (Mock CPM)
F
PO vs Diacetyl
Mock vs SB
Mock vs VA
532
15
109
20 Common (UP)
78
35
84
Odds Ratio
5 15 25
6 x 10-11
2 x 10-65
diacetyl
- -
1 x 10-52
SB
SB
VA
G
Common (UP)
response to cAMP
response to organo-phosphorous
response to purine-containing compound
osteoblast differentiation
cellular response to calcium ion
p-value
6e-04
4e-04
2e-04
Gene Count
H
Common (DOWN)
striated muscle contraction
cardiac muscle contraction
muscle contraction
heart contraction
heart process
muscle system process
regulation of muscle system process
blood circulation
p-value
2.5e-06
2.0e-06
1.5e-06
1.0e-06
5.0e-07
Gene Count

Figure 4

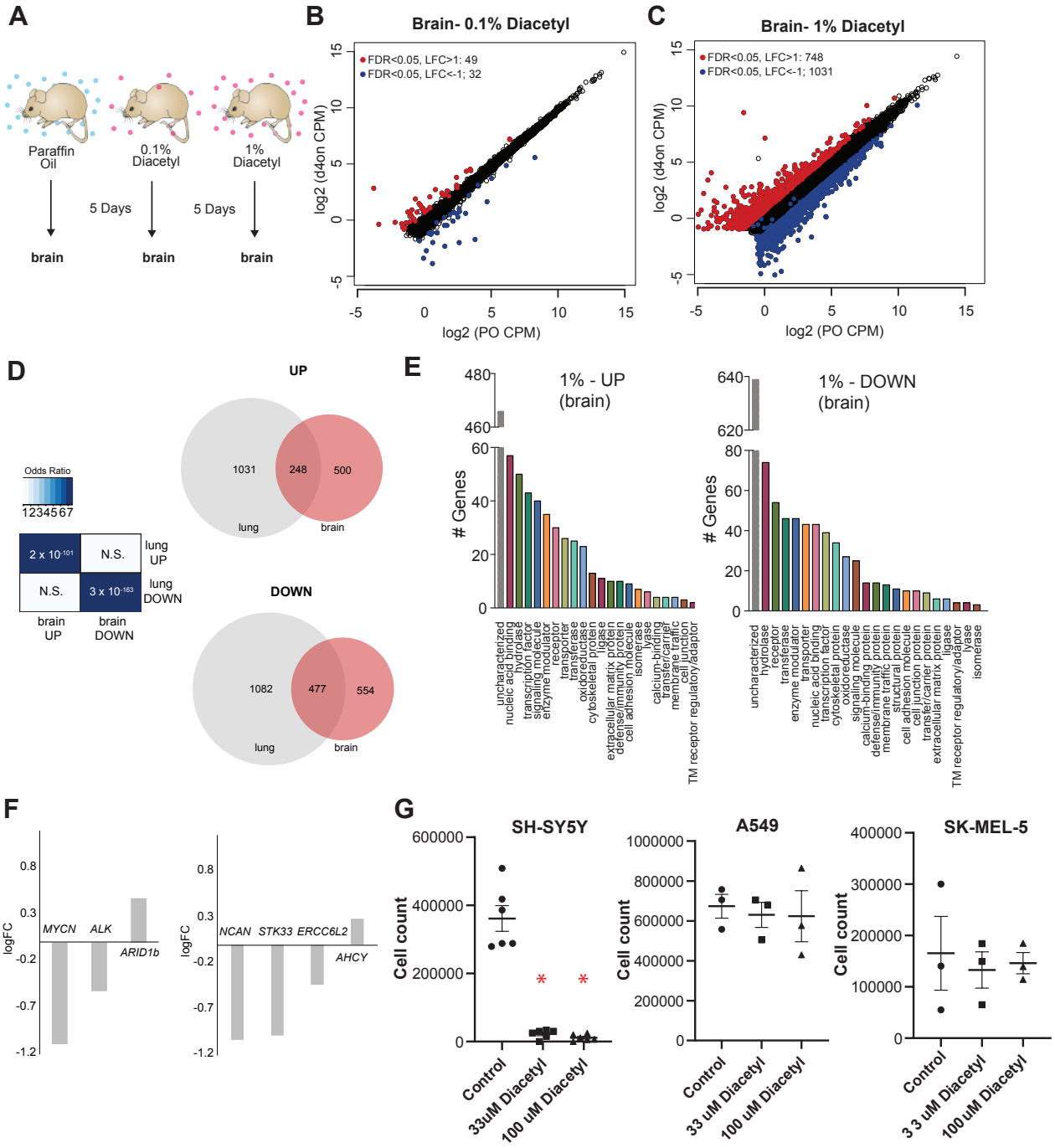
A
Paraffin Oil
0.1% Diacetyl
1% Diacetyl
5 Days
5 Days
brain
brain
brain
B
Brain- 0.1% Diacetyl
FDR<0.05, LFC>1: 49
FDR<0.05, LFC<-1; 32
log2 (d4on CPM)
log2 (PO CPM)
C
Brain- 1% Diacetyl
FDR<0.05, LFC>1: 748
FDR<0.05, LFC<-1; 1031
log2 (d4on CPM)
log2 (PO CPM)
D
Odds Ratio
1234567
2 x 10-101
N.S.
N.S.
3 x 10-163
lung UP
lung DOWN
brain UP
brain DOWN
UP
1031
248
500
lung
brain
DOWN
1082
477
554
lung
brain
E
1% - UP (brain)
Genes
uncharacterized
nucleic acid binding
hydrolase
transcription factor
signaling molecule
enzyme modulator
receptor
transporter
transferase
oxidoreductase
cytoskeletal protein
ligase
extracellular matrix protein
defense/immunity protein
cell adhesion molecule
isomerase
lyase
calcium-binding
transfer/carrier
membrane traffic
cell junction
TM receptor regulatory/adaptor
1% - DOWN (brain)
Genes
uncharacterized
hydrolase
receptor
transferase
enzyme modulator
transporter
nucleic acid binding
transcription factor
cytoskeletal protein
oxidoreductase
signaling molecule
calcium-binding protein
defense/immunity protein
membrane traffic protein
structural protein
cell adhesion molecule
cell junction protein
transfer/carrier protein
extracellular matrix protein
ligase
TM receptor regulatory/adaptor
lyase
isomerase
F
logFC
MYCN
ALK
ARID1b
logFC
NCAN
STK33
ERCC6L2
AHCY
G
SH-SY5Y
Cell count
Control
33uM Diacetyl
100 uM Diacetyl
A549
Cell count
Control
33 uM Diacetyl
100 uM Diacetyl
SK-MEL-5
Cell count
Control
3 3 uM Diacetyl
100 uM Diacetyl

Figure 5

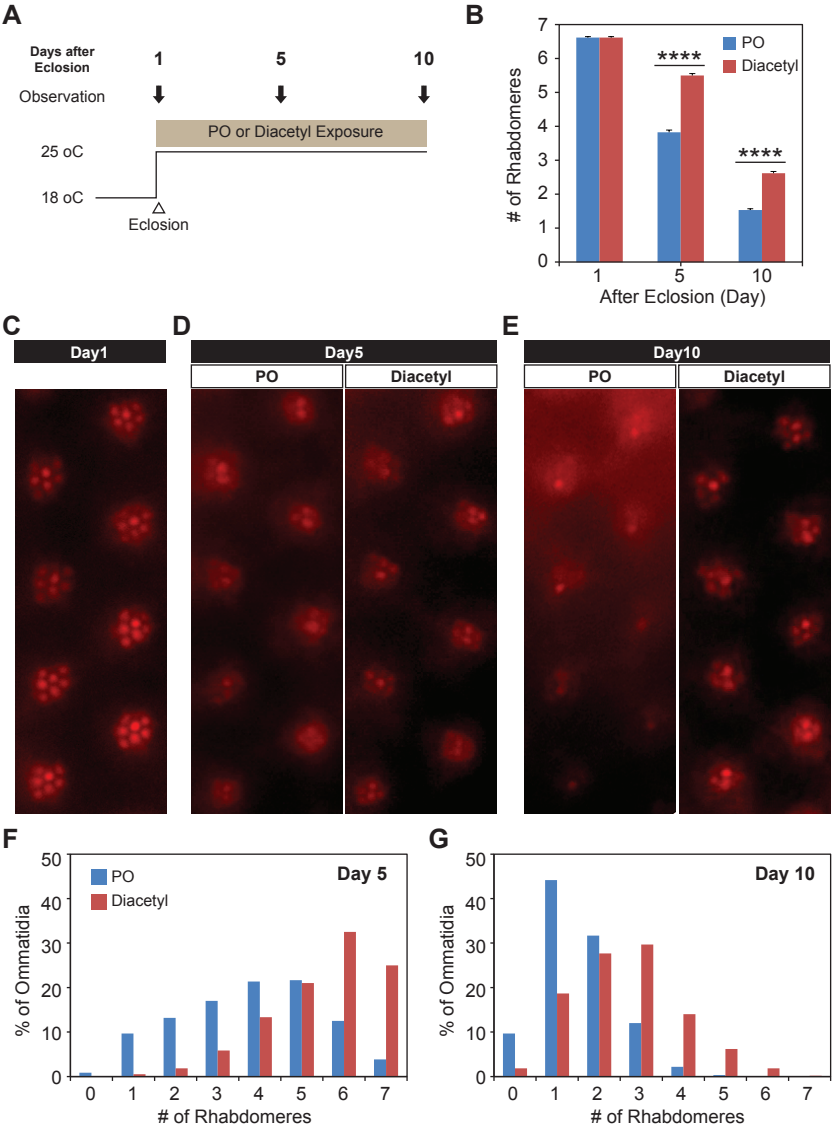
A
Days after Eclosion
1
5
10
Observation
PO or Diacetyl Exposure
25 oC
18 oC
Eclosion
B
PO
Diacetyl
****
****
# of Rhabdomeres
After Eclosion (Day)
C
Day1
D
Day5
PO
Diacetyl
E
Day10
PO
Diacetyl
F
PO
Diacetyl
Day 5
% of Ommatidia
# of Rhabdomeres
G
Day 10
% of Ommatidia
# of Rhabdomeres

Figure 6